HARMONI at ELT: wavefront control in SCAO mode

Charlotte Bond, Jean-François Sauvage, Noah Schwartz, Nicolas Levraud, Vincent Chambouleyron, Carlos Correia, Thierry Fusco, Benoit Neichel

HARMONI at ELT: Wavefront control in SCAO mode

Charlotte Z. Bond[a], Jean-François Sauvage[b], Noah Schwartz[a], Nicolas Levraud[c], Vincent Chambouleyron[c], Carlos Correia[d,e], Thierry Fusco[b], and Benoit Neichel[c]

[a]UK Astronomy Technology Centre, Blackford Hill, Edinburgh EH9 3HJ, United Kingdom
[b]ONERA, 29 avenue de la Division Leclerc, 92322 Châtillon, France
[c]Aix Marseille Univ, CNRS, CNES, LAM, Marseille, France
[d]Space ODT - Optical Deblurring Technologies, Portugal
[e]INESTEC, FEUP, Porto, Portugal

ABSTRACT

HARMONI is the first light visible and near-IR integral field spectrograph for the ELT. It covers a large spectral range from 450nm to 2450nm with resolving powers from 3500 to 18000 and spatial sampling from 60mas to 4mas. It can operate in two Adaptive Optics (AO) modes - SCAO (including a High Contrast capability) and LTAO - or with NOAO. The project is preparing for Final Design Reviews.

The SCAO system for HARMONI is based on a pyramid wavefront sensor (PWFS) operating in the visible (700 – 1000 nm). Previous implementations on very large telescopes have demonstrated the challenges associated with optimising PWFS performance on-sky, particularly when operated at visible wavelengths. ELT operation will pose further challenges for AO systems, particularly related to the segmentation of the telescope and the control of badly seen 'petal modes'. In this paper we investigate these challenges in the context of the HARMONI SCAO system. We present the results of end-to-end simulations of our baseline approach, using a coupled control basis to avoid the runaway development of petal modes in the control loop. The impact of key parameters are investigated and methods for optical gain compensation and optimisation of the control basis are presented. We discuss recent updates to the control algorithms and demonstrate the possibility of improving performance using a form of super resolution. Finally, we report on the expected performance across a range of conditions.

Keywords: Pyramid wavefront sensing, Extremely Large Telescope, Adaptive Optics

1. INTRODUCTION

HARMONI is the first light visible and near-IR integral field spectrograph for the European Extremely Large Telescope (ELT).[1,2] HARMONI works in several different modes depending on the resolution and sky-coverage requirements of the observation.[3,4] These are a seeing limited mode (NOAO); laser tomographic AO mode (LTAO); and a single conjugate AO mode (SCAO). A high contrast mode (HCAO) is also available as an extension of the SCAO mode. The SCAO mode provides high performance but limited sky-coverage, whilst the LTAO mode combines medium performance with good sky-coverage. In this paper we will focus on the SCAO mode and some of the challenges associated with SCAO operation on the ELT.

The SCAO mode is required to provide high resolution AO correction with at least 70% Strehl ratio in K-band for median conditions. In section 2 we present an overview of the SCAO system. We face a number of challenges to reach the required performance. One of the critical issues is the fragmentation of the pupil due to the telescope support structure and the consequences this has for the AO system, namely an insensitivity to the petal piston modes of the telescope. This effect is described in section 3 along with reporting on the extensive work carried out to mitigate this effect in HARMONI using a specialised control basis. In section 4 we report on other aspects of wavefront control, specifically the processing of the PWFS signals and compensation of optical gain. Finally we summarise the HARMONI SCAO performance in section 5.

Further author information: (Send correspondence to C. Z. Bond)
E-mail: charlotte.bond@stfc.ac.uk

2. HARMONI IN SCAO MODE

2.1 SCAO loops

Figure 1 illustrates the key components of the HARMONI SCAO system. Light is provided by a natural guide star (NGS). In SCAO mode the longer wavelengths ($> 1000\,\mathrm{nm}$) are sent to the science instrument (INS). The main AO loop consists of an I band ($700-1000\,\mathrm{nm}$) Pyramid WFS (PWFS) and the ELT correctors (M4 and M5). This loop controls up to 4000 modes at high speed (baseline 500 Hz) to correct for atmospheric turbulence. The shorter, bluer wavelengths are sent to a Shack-Hartmann WFS. This forms part of a low order loop which, along with a 9×9 low order deformable mirror (LODM), slowly corrects for non-common path aberrations (NCPA) between the instrument and PWFS. The combination of the low order loop and main AO loop allow the system to simultaneously flatten the wavefront for the science path and PWFS, whilst amy NCPA is compensated by applying reference slopes to the Shack-Hartmann WFS. This is preferable to compensating the NCPA through PWFS reference slopes as the PWFS can be pushed its non-linear regime and any offset from zero can cause a loss in sensitivity.

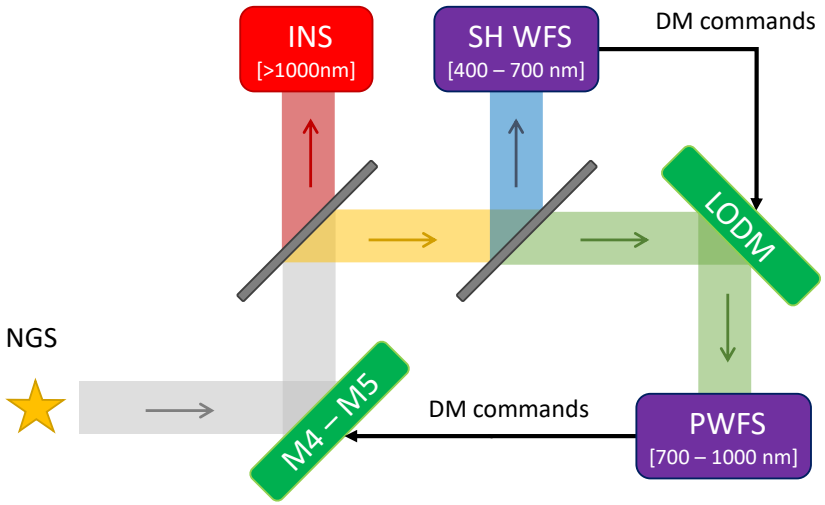

Figure 1. Illustration of the key components of the HARMONI SCAO system.

In addition to the two AO loops outlined above we implement several pupil stabilization loops. These are used to position the pupil on the PWFS and maintain registration between the actuators of the high order DM (M4) and the PWFS pixels. This is achieved by adjusting the lateral position, rotation and magnification of the PWFS image on the detector.

The High Contrast (HCAO) mode of HARMONI is an extension of the SCAO mode.[5] As well as the loops described above a Zernike WFS provides measurements of quasi-static NCPA. These measurements are fed back to the SCAO low order loop for low order NCPA correction and to the main AO loop for high order NCPA correction. The high order component is expected to be small and so will not impact the performance of the PWFS.

In this paper we deal with the standard SCAO mode and specifically with the main AO loop. The qualitative conclusions drawn here apply to the HCAO mode as well, with the stipulation that the HCAO mode is expected to be used in in conditions better than the median conditions used for the analysis presented here.

2.2 SCAO parameters

In this paper we analyse the performance of the HARMONI SCAO system through end-to-end simulations using OOMAO (Object Oriented Matlab Adaptive Optics toolbox).[6] Here we summarise the key SCAO parameters

Table 1. Baseline HARMONI SCAO simulation parameters

AO system	
Frame rate	500 Hz
PWFS sampling	100×100
PWFS band	I-band
PWFS modulation	$3\frac{\lambda}{D}$
DM correction	4000 KL modes

Atmosphere	
Median seeing	0.65”
Wind speed	8 m/s
Zenith angle	30°

used throughout. Unless otherwise stated these are the default system and atmospheric simulation parameters.

In this paper we focus on the performance of the main AO loop with respect to the correction of atmospheric turbulence. Other errors are not included in the simulations presented here but are accounted for in the wider error budget to determine the final image quality. For example, telescope phasing errors are not included in these simulations but are reported on elsewhere.[7]

3. CONTROLLING THE PETAL MODES IN SCAO MODE

3.1 Pupil fragmentation and the petal modes

Part of the support structure of the ELT includes six 50 cm wide spiders. The spiders effectively split the pupil into 6 segments, as shown in figure 2. This fragmentation of the pupil can cause a problem for AO systems using gradient-like sensors, such as the Shack-Hartmann or modulated PWFS, as they are insensitive to piston. This is not a problem for systems with non-fragmented pupils as the global piston has no impact on the final image quality. However, in the fragmented case gradient-like sensors become insensitive to the piston mode for each individual segment, the so called *petal piston modes* or *petal modes* (see figure 2). These modes need to be well corrected to achieve near diffraction limited image quality. This is a particular issue for ELT-scale systems where the spiders are typically wider than a single sampling element on the WFS. For example, in the HARMONI SCAO mode the PWFS pixel size is 38 cm, compared with a spider width of 50 cm.

For a PWFS the signal from the petal mode is concentrated in the light diffracted around the spider. In simulation we can close the loop on the petal modes in isolation. However, in the presence of atmospheric turbulence the petal modes become hard to control. For median seeing and using a visible PWFS the petal modes typically stabilize at integer multiples of half the wavefront sensing wavelength. This effect is often referred to as *petalling* or the *island effect*. The greater the turbulence the harder it becomes to control the petal modes and so the petalling effect is greater for WFSs working at shorter wavelengths where the effective seeing is greater. Examples of the impact of petalling on the residual wavefront and PSF are given in section 3.2.

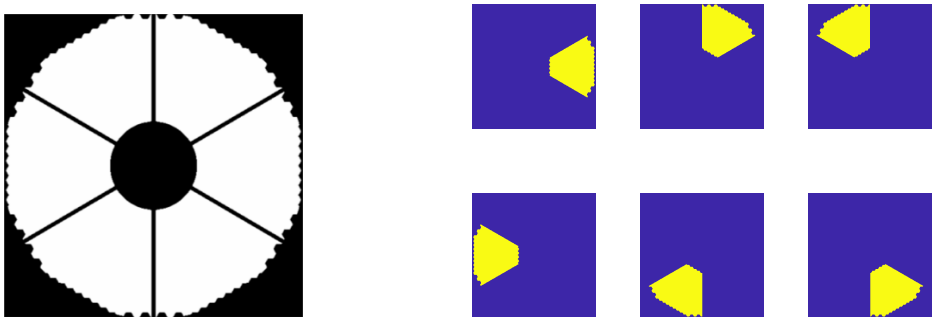

Figure 2. Pupil fragmentation and the petal modes. Left: Diagram of the footprint of the ELT pupil, including the spiders. Right: The petal piston modes of the ELT.

3.2 Edge Actuator Coupling

Often in AO systems modes with low sensitivity can be filtered out during the reconstruction process. A classic example is the waffle mode in systems using a Shack-Hartmann WFS. However, the petal modes have a significant contribution in the atmosphere across a whole range of spatial frequencies and so must be corrected to achieve high resolution. To avoid the development of large petal modes in the AO residuals the HARMONI SCAO system employs a reduced modal basis to restrict the ability of the DM to produce the pure petal modes. This is achieved by pairing actuators either side of the spider and coupling them together. We refer to this as Edge Actuator Coupling (EAC).[8] The process is illustrated in figure 3.

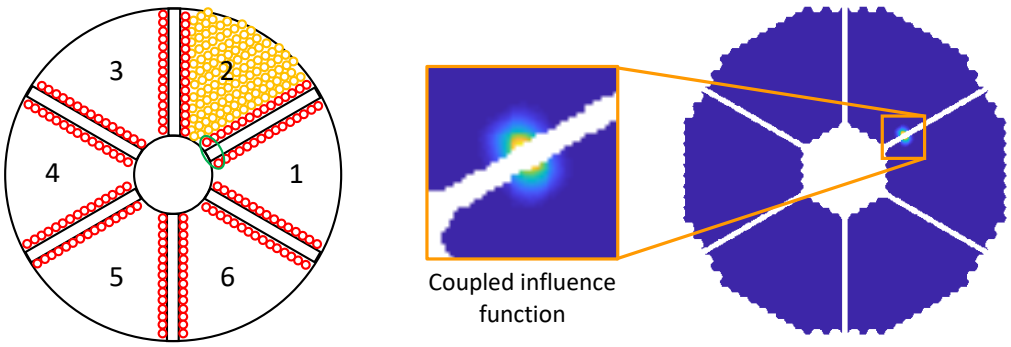

Figure 3. Illustration of Edge Actuator Coupling.[8] Left: actuators either side of the spiders are paired together. Right: influence function of coupled edge actuators.

By coupling actuators across the spider the DM is still able to create petal-like modes, but cannot create the sharp discontinuities under the spider. This allows for correction of the majority of the petal content in the turbulence but uses modes which are better seen by the PWFS. Simulations of the HARMONI SCAO system have demonstrated that the use of EAC avoids the development of large petal errors in closed loop. This is illustrated in figure 4 where one instance of the closed loop residual wavefront is shown, both with (left) and without EAC (right). The corresponding K-band PSFs are shown in figure 5. Without EAC a large petal error is present, corresponding to $\sim 400\,\mathrm{nm}$ rms and resulting in a highly distorted PSF. With EAC the wavefront does not exhibit large petal errors, with an average residual wavefront error of 125 nm and a well corrected PSF (close to 90% Sterhl in K-band).

Figure 6 shows a plot of the simulated closed loop wavefront rms vs. time. The HARMONI SCAO baseline using EAC is shown in purple and for comparison a reference case without spiders is shown (red), as well as the case with spiders and without EAC (yellow). Here we can see that without EAC not only is the average

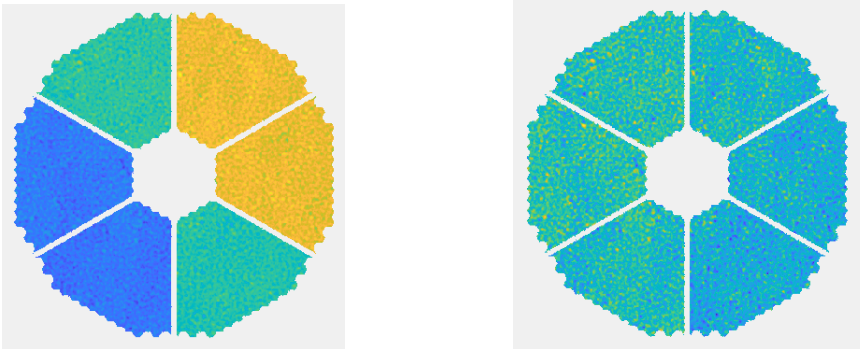

Figure 4. Examples of the closed loop wavefront residual for simulations of the HARMONI SCAO system for median conditions. The residual is shown for the case without EAC (left) and with EAC (right).

Figure 5. Examples of the closed loop short exposure K-band PSF for simulations of the HARMONI SCAO system for median conditions. The PSF is shown for the case without EAC (left) and with EAC (right). These PSFs correspond to the respective residual wavefronts shown in figure 4

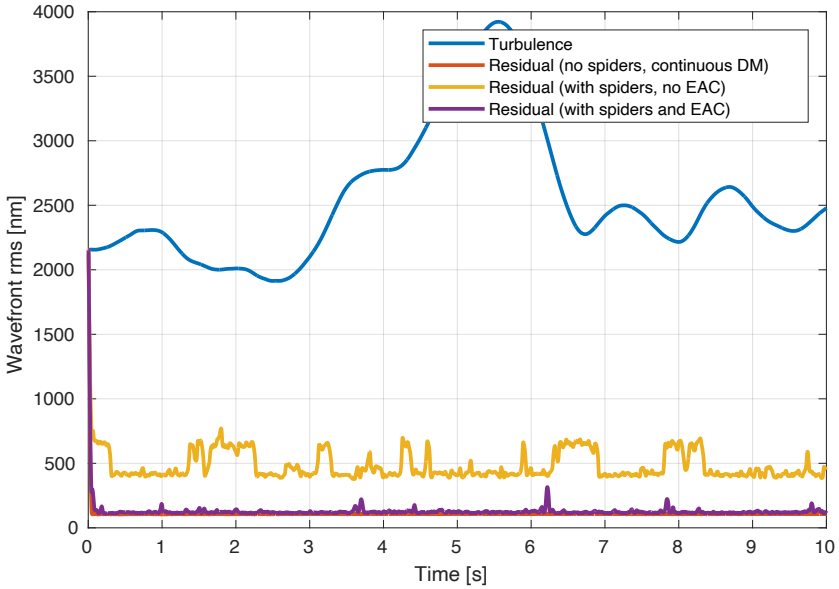

Figure 6. Simulated closed loop performance (residual wavefront rms) of the HARMONI SCAO system vs. time for median conditions.

residual rms much higher, but that the system oscillates between different states. This occurs when the different petal modes jump between different multiples of $\frac{\lambda}{2}$. The result with EAC remains stable around 120 nm rms. However, we do see some short-term peaks in the residual caused by flare ups of the petal modes. As these flare ups are short lived and their average contribution is within our error budget for median conditions this behaviour is acceptable as the HARMONI SCAO baseline. However, continued analysis is anticipated to further improve performance and stability.

The results presented in this section also make use of a modified DM basis defined by an inter-actuator coupling of 40%. This basis is described in more detail in section 3.3.

3.3 SCAO control basis

In addition to using EAC the HARMONI SCAO system defines a modified DM basis from a linear combination of the M4 influence functions. The goal is to produce a set of influence functions for the control basis which more closely represent Gaussian influence functions and, together with the EAC method, optimise performance. The basis is defined by a coupling coefficient, c, which defines inter-actuator coupling at a distance of 0.5 m from the

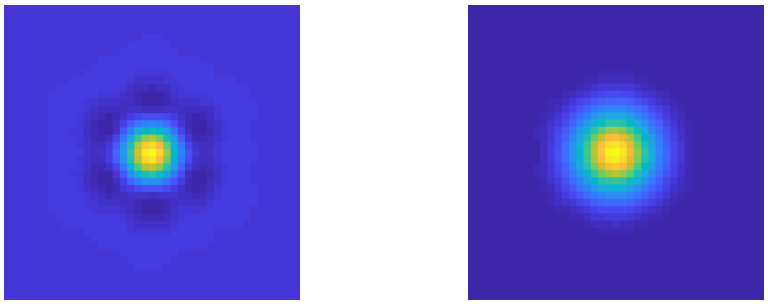

Figure 7. Example influence functions used in HARMONI SCAO simulations. Two examples are shown, the M4 influence function (left) and a 40% coupled influence function.

master actuator. Figure 7 shows examples of an M4 influence function and a modified influence function (with 40% coupling). EAC is then applied to this modified basis. Finally this basis is used to compute the modal control basis, a set of Karhunen–Loève (KL) modes. The HARMONI SCAO system will control up to 4000 KL modes depending on the observing conditions.

Figure 8 shows a plot of the average residual wavefront rms vs. the inter-actuator coupling. A coupling of 0 signifies the original M4 influence functions. The variation in performance for different couplings is dominated by the residual petal modes. The performance is optimized for a coupling of $\sim 50\%$. This is a balance between smaller coupling, where the impact of the EAC to smooth the discontinuities is reduced, and larger couplings where the next row of actuators can produce a sharp discontinuity. For the HARMONIC SCAO baseline a coupling of 40% was chosen.

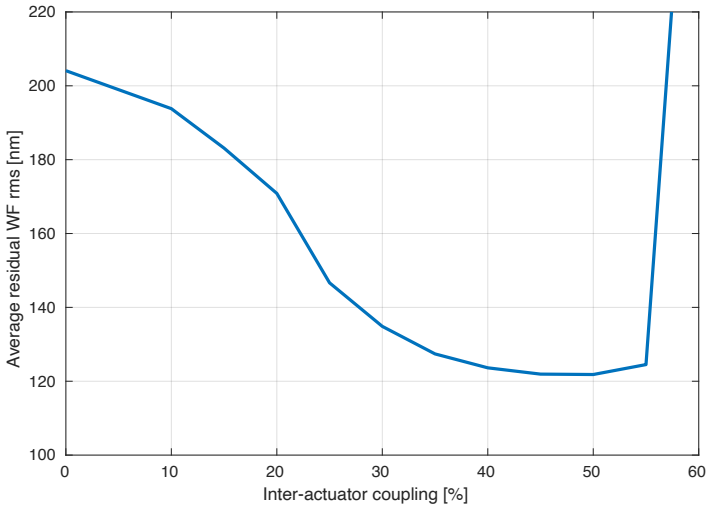

Figure 8. Simulated closed loop performance (average residual wavefront rms) of the HARMONI SCAO system vs. inter-actuator coupling for median conditions.

3.4 Impact of modulation

One of the key parameters determining the sensitivity to the petal modes of the HARMONI SCAO system is the modulation of the PWFS. Figure 9 shows the impact of modulation on the average residual wavefront rms. The results are shown both with and without optical gain compensation (see section 4.2). For small modulation the sensitivity to the petal modes is increased as more light is diffracted around the spider. However, this must be balanced against other non-linear effects that begin to dominate at low modulation ($< 1.5\frac{\lambda}{D}$ in

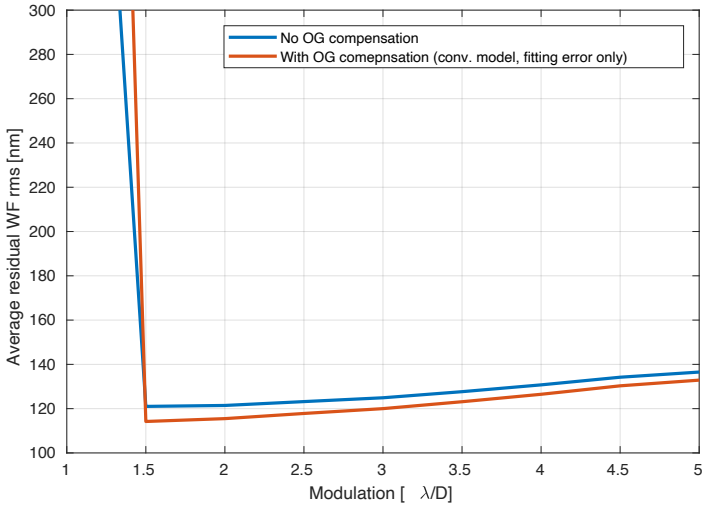

Figure 9. Simulated closed loop performance (average residual wavefront rms) of the HARMONI SCAO system vs. PWFS modulation in median conditions.

median conditions). To give a margin for such non-linear effects the HARMONI SCAO baseline modulation is $3\frac{\lambda}{D}$. However, for high contrast operation, where we will be operating under better than median conditions the modulation is likely to be reduced.

4. WAVEFRONT RECONSTRUTION

4.1 Processing the WFS signals

The raw PWFS signal is the camera frame of 4 pupil images after pre-processing (background subtraction, flat fielding etc.). There are different algorithms which can then be applied to produce a set of signals appropriate for wavefront sensing. For the HARMONI SCAO system we have considered two methods, the *slopes* and the *pseudo-intensities*.

The slopes are analogous to the x and y slopes of classical gradient sensors such as the Shack-Hartmann WFS. A quad cell formula is applied to the 4 pupil images to produce 2 slope maps:

$$S_x = \frac{I_1 + I_3 - I_2 - I_4}{I_{norm}} \tag{1}$$

$$S_y = \frac{I_1 + I_2 - I_3 - I_4}{I_{norm}} \tag{2}$$

where I_n refer to the PWFS 4 pupil images ($n = 1, 2, 3, 4$) and I_{norm} is the total intensity. The pseudo-intensities are the normalized PWFS frame with a reference image corresponding to a flat wavefront removed. For both the slopes and pseudo-intensities the valid pixels are selected through an intensity threshold.

There are two aspects we considered when comparing these two methods. The first is the computational burden. The size of the WFS data and reconstructors depends on the processing method. For the slopes this is $2N$ whilst for the pseudo-intensities this is $4N$ (where N is the number of valid pixels in a single pupil image). In the case of the HARMONI SCAO system the Real Time Controller (RTC) splits the reconstruction process over several nodes which compute a subset of the reconstruction in parallel.[9] To modify the baseline from slopes to pseudo-intensities requires 1 extra node to continue to meet the 2 frame delay latency requirements. This is easily achievable for HARMONI as the number of nodes is determined by the larger computational burden of the LTAO mode.

The second aspect we consider is the impact on performance of the relative position of the 4 PWFS pupil images. This is determined by the PWFS optics. Typically a PWFS is designed so that each pupil image is sampled at the same locations in each pupil, i.e. the pupil images are separated by an integer number of pixels. However, this requires very tight requirements on the PWFS optics. Simulation studies have shown that the slopes method can become insensitive to higher spatial frequencies if the pupil separations deviate from an integer as the combination of the shifted pupil images smears the wavefront information. If this deviation is too large (for a single pupil image the maximum shift is 0.5 pixels) the performance degrades and the loop can become unstable. The pseudo-intensity method does not exhibit such behaviour as there is no combination of the pupil images. In fact the pseudo-intensities benefit from different sampling of 4 pupil images as this provides more information of the wavefront, a form of *super resolution*.[10] The impact of the relative pupil positions on HARMONI SCAO performance is shown in figure 10 for both methods. In this case the shift is a radial shift of all 4 pupils from the centre, so a shift of 0.25 pixels is equivalent to a shift of 0.5 pixels for an individual pupil (the maximum relative shift). This plot illustrates the degrading and eventually unstable performance when using the slopes as well as the improvement in performance for pseudo-intensities with increasing pupil shift. As a result of such simulation studies pseudo-intensities are now the baseline for the HARMONI SCAO system. This allows us to avoid very tight requirements on the PWFS optics and, depending on the final positions of the pupil images, potentially benefit from super-resolution.

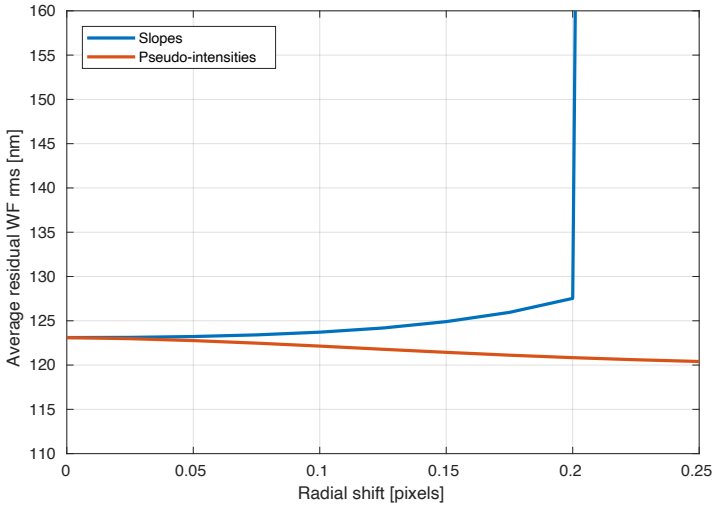

Figure 10. Simulated closed loop performance (average residual wavefront rms) of the HARMONI SCAO system vs. relative pupil positioning (shift). The results are shown for two signal processing methods: slopes and pseudo-intensities.

4.2 Optical gain compensation

The high sensitivity of the PWFS comes at the expense of a small linear range. One consequence of this is a mismatch between the behaviour during calibration and operation. Typically the system is calibrated using a diffraction limited PSF, whereas the system is operated with an AO corrected PSF. Consequently the response of the PWFS to an incoming wavefront differs between calibration and operation. If no adjustments to the reconstructor are made to compensate for this the wavefront is underestimated during on-sky operation. This is often referred to as the *optical gain* effect.

Extensive work on the topic of optical gains for PWFSs have shown that the effect can be well described by a gain applied to each spatial mode.[11] These optical gains are < 1 and will depend on the seeing, quality of the AO correction, modulation, and wavefront sensing wavelength. In the case of the HARMONI SCAO mode, we are carrying out the wavefront sensing in the visible (I-band) and so the optical gain is expected to have a significant impact, especially at larger seeing. The fundamental loss in sensitivity can not be re-captured. However, we can

address the mismatch between calibrating and operating behaviour. If we can estimate the optical gain we can modify our reconstructor to optimise performance on-sky:

$$\mathrm{CM}_{sky} = \frac{1}{G_{opt}}\mathrm{CM}_{calib} \tag{3}$$

where G_{opt} is the optical gain and CM_{calib} is the original reconstructor computed from the calibrated interaction matrix. For HARMONI we use the convolutional model[11,12] to compute the optical gains. For each spatial mode, ϕ_i, the gain is computed:

$$G_{opt} = \frac{\langle \mathrm{IR}_{sky} \star \phi_i | \mathrm{IR}_{calib} \star \phi_i \rangle}{\langle \mathrm{IR}_{calib} \star \phi_i | \mathrm{IR}_{calib} \star \phi_i \rangle} \tag{4}$$

$\star$ denotes a convolution and IR_{calib} and IR_{sky} are the impulse response for calibration and on-sky operation respectively. The impulse response depends on the complex mask describing the pyramid operation, m, and a modulation function Ω:[13]

$$\mathrm{IR} = 2\mathrm{Im}(\widehat{\bar{m}}(\widehat{m} \star \widehat{\Omega})) \tag{5}$$

Ω depends on the PSF and modulation and so it is this quantity that determines the optical gain:

$$\Omega = \mathrm{PSF} \star \omega \tag{6}$$

where ω is the modulation weighting function. The PSF will be the diffraction limited PSF for IR_{calib} and the AO corrected PSF for IR_{sky}. Ideally a focal plane camera close to the PWFS could provide a measurement of the PSF, or Ω directly if it were placed after the modulator. However, for the HARMONI SCAO system there is no such camera and so the PSF must be estimated from the AO telemetry. Simulation of the system has determined that the fitting error dominates the optical gain. therefore, in order to estimate the optical gain a PSF is reconstructed using only the fitting error and used as the input to the convolutional model.

In figure 11 the residual wavefront rms vs. seeing is plotted for the case of no optical gain compensation and using the fitting only optical gain compensation described above. The result is well within our requirements for median seeing and greatly improves the performance at larger seeing. For this approach to optical gain compensation the only input is an estimate of r_0 and the PWFS modulation. Simulations incorporating errors on the r_0 estimate have shown that, to comply with the HARMONI SCAO error budget, r_0 must be accurate to within $-10\% < r_0 < 30\%$. The range is non-symmetric as if r_0 is underestimated a larger compensatory

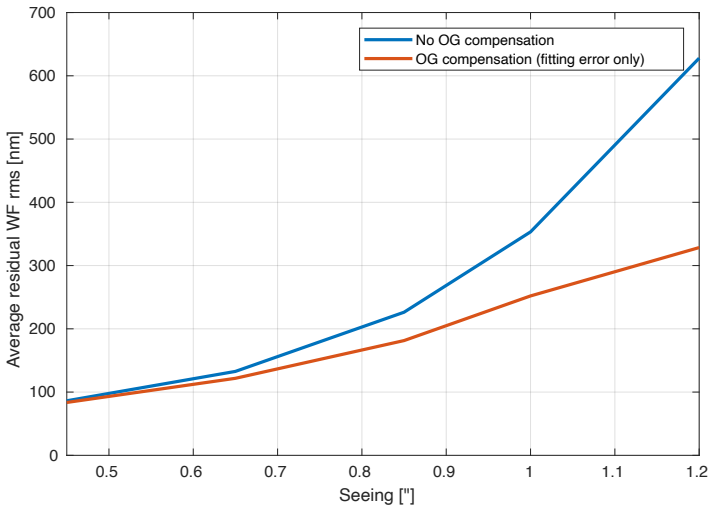

Figure 11. Simulated closed loop performance (average residual wavefront rms) of the HARMONI SCAO system vs. seeing. Results are shown with and without optical gain compensation.

gain is applied, which can more quickly lead to instabilities. If r_0 is over-estimated the optical gain is not quite compensated and the response of the system is slower. Although this degrades the performance it is less likely to lead to instability.

5. BASELINE H-SCAO PERFORMANCE

. In this section we present the baseline HARMONI SCAO performance. This incorporates the basis defined in section 3.2 and the wavefront reconstruction algorithms outlined in section 4. The baseline parameters are defined in section 2.2.

Firstly we show the performance (K-band Strehl ratio) vs. Fried parameter (r_0) in the high flux regime. This is shown in figure 12. Good performance is obtained over a range of r_0, with the implementation of the optical gain compensation enabling reasonable performance even for $r_0 < 10\,\mathrm{cm}$. Figure 13 shows the performance vs. flux on the PWFS for median conditions. The performance remains robust until the flux drops to ~ 10 photons per pixel per frame, at which point the performance begins to decrease. However, we still maintain a decent level of correction up to ~ 1 photon per pixel per frame.

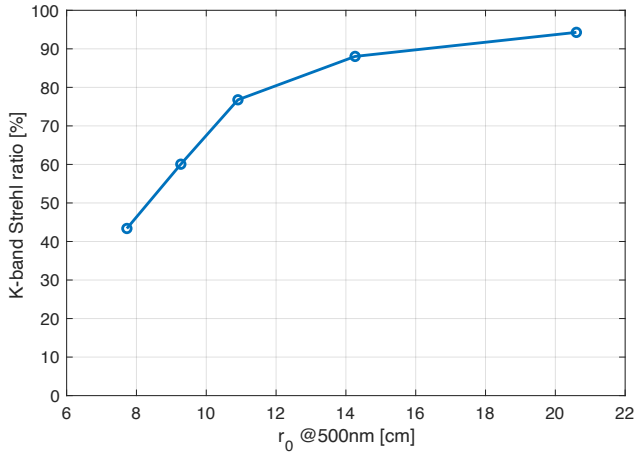

Figure 12. Simulated closed loop performance (K-band Strehl) of the HARMONI SCAO system vs. r_0 in the high flux regime.

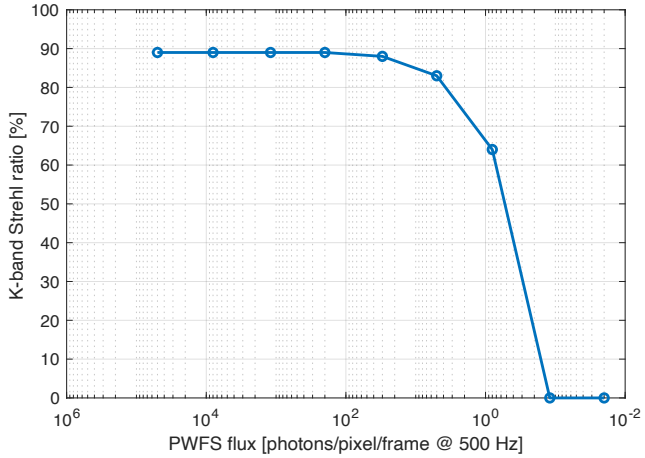

Figure 13. Simulated closed loop performance (K-band Strehl) of the HARMONI SCAO system vs. flux for median seeing conditions.

The performance shown here uses the HARMONI SCAO baseline: a frame rate of 500 Hz; controlling 4000 modes; a PWFS modulation of $3\frac{\lambda}{D}$; and nominal gains. However, optimisation of the SCAO parameters and controllers, depending on the observing conditions, is expected to improve on this baseline performance.

6. CONCLUSION

In this paper we have presented the results of end-to-end simulations of the HARMONI SCAO mode, focusing on the behaviour and challenges associated with the main AO loop. We have shown how the large spiders of the ELT cause an insensitivity to the petal modes of the telescope and demonstrated the use of Edge Actuator Coupling to prevent the build up of large petal errors in closed loop. Combining Edge Actuator Coupling with a modified DM basis greatly improves performance. We also present recent modifications to the baseline wavefront reconstruction process. Specifically we will employ the pseudo-intensity method of processing the PWFS data, providing robustness against the positioning of the PWFS pupil images on the detector. We also reported on our approach to optical gain compensation using the convolutional model. Finally we have presented the baseline HARMONI SCAO performance with respect to Fried parameter and flux, showing good performance across a range of observing conditions.

Our next steps are to further optimise the reconstructors and AO parameters for different observing conditions. We will also include effects evolving from the telescope environment into our simulations, such as the low wind effect and phasing errors. Finally we will work with the AO control system team to implement and test the algorithms and reconstruction methods in real time.

ACKNOWLEDGMENTS

HARMONI is an instrument designed and built by a consortium of British, French, and Spanish institutes in collaboration with ESO. This work benefited from the support of the the French National Research Agency (ANR) with WOLF (ANR-18-CE31-0018), APPLY (ANR-19-CE31-0011) and LabEx FOCUS (ANR-11-LABX-0013); the Programme Investissement Avenir F-CELT (ANR-21-ESRE-0008), the Action Spécifique Haute Résolution Angulaire (ASHRA) of CNRS/INSU co-funded by CNES, the ORP H2020 Framework Programme of the European Commission's (Grant number 101004719) and STIC AmSud (21-STIC-09).

REFERENCES

[1] Thatte, N. A., Clarke, F., et al., "HARMONI: The first light integral field spectrograph for the E-ELT," in [*Ground-based and Airborne Instrumentation for Astronomy V*], *Proc. SPIE* **9147** (2014).

[2] Thatte, N. A., Bryson, I., et al., "HARMONI: First light spectroscopy for the ELT: instrument final design and quantitative performance predictions," in [*Ground-based and Airborne Instrumentation for Astronomy VIII*], *Proc. SPIE* **11447** (2020).

[3] Thatte, N. A., Clarke, F., et al., "The E-ELT first light spectrograph HARMONI: capabilities and modes," in [*Ground-based and Airborne Instrumentation for Astronomy VI*], *Proc. SPIE* **9908** (2016).

[4] Neichel, B., Fusco, T., et al., "The adaptive optics modes for HARMONI: from Classical to Laser Assisted Tomographic AO," in [*Adaptive Optics Systems V*], *Proc. SPIE* **9909** (2016).

[5] Carlotti, A., Hénault, F., et al., "System analysis and expected performance of a high-contrast module for HARMONI," in [*Ground-based and Airborne Instrumentation for Astronomy VII*], *Proc. SPIE* **10702** (2018).

[6] Conan, R. and Correia, C., "Object-oriented Matlab adaptive optics toolbox," in [*Adaptive Optics Systems IV*], *Proc. SPIE* **9148** (2014).

[7] Schwartz, N. et al., "Design of the HARMONI Pyramid WFS module," *6th International Conference on Adaptive Optics for Extremely Large Telescopes* (2019).

[8] Schwartz, N., Sauvage, J.-F., et al., "Analysis and mitigation of pupil discontinuities on adaptive optics performance," in [*Adaptive Optics Systems VI*], *Proc. SPIE* **10703** (2018).

[9] Younger, E. J., Dimoudi, S., et al., "HARMONI: first light spectroscopy for the ELT: design of the AO control system," in [*Software and Cyberinfrastructure for Astronomy VI*], *Proc. SPIE* **11452** (2020).

[10] Fusco, T. et al., "Key wavefront sensors features for laser-assisted tomographic adaptive optics systems on the Extremely Large Telescope," *Journal of Astronomical Telescopes, Instruments, and Systems* (2022).

[11] Chambouleyron, V. et al., "Pyramid wavefront sensor optical gains compensation using a convolutional model," *A&A* (2020).

[12] Fauvarque, O. et al., "Kernel formalism applied to fourier-based wave-front sensing in presence of residual phases," *J. Opt. Soc. Am. A* (2019).

[13] Chambouleyron, V. et al., "Focal-plane-assisted pyramid wavefront sensor: Enabling frame-by-frame optical gain tracking," *A&A* (2021).